Bioprinting 3D cell-laden hydrogel microarray for screening human periodontal ligament stem cell response to extracellular matrix

2015 Biofabrication 7 044105

(http://iopscience.iop.org/1758-5090/7/4/044105)

Biofabrication

PAPER

Bioprinting 3D cell-laden hydrogel microarray for screening human periodontal ligament stem cell response to extracellular matrix

Yufei Ma[1,2], **Yuan Ji**[1,2], **Guoyou Huang**[1,2], **Kai Ling**[2,3], **Xiaohui Zhang**[1,2] **and Feng Xu**[1,2]

[1] The Key Laboratory of Biomedical Information Engineering, Ministry of Education, School of Life Science and Technology, Xi'an Jiaotong University, Xi'an 710049, People's Republic of China
[2] Bioinspired Engineering and Biomechanics Center (BEBC), Xi'an Jiaotong University, Xi'an 710049, People's Republic of China
[3] State Key Laboratory for Mechanical Structure Strength and Vibration, Xi'an Jiaotong University, Xi'an 710049, People's Republic of China

E-mail: xiaohuizhang@mail.xjtu.edu.cn **and** fengxu@mail.xjtu.edu.cn

RECEIVED
15 May 2015

REVISED
13 August 2015

ACCEPTED FOR PUBLICATION
11 November 2015

PUBLISHED
22 December 2015

Keywords: 3D cell printing, bioprinting, periodontal ligament stem cells, extracellular matrix, hydrogel

Abstract

Periodontitis is an inflammatory disease negatively affecting up to 15% of adults worldwide. Periodontal ligament stem cells (PDLSCs) hold great promises for periodontal tissue regeneration, where it is necessary to find proper extracellular matrix (ECM) materials (e.g., composition, concentration). In this study, we proposed a bioprinting-based approach to generate nano-liter sized three-dimensional (3D) cell-laden hydrogel array with gradient of ECM components, through controlling the volume ratio of two hydrogels, such as gelatin methacrylate (GelMA) and poly (ethylene glycol) (PEG) dimethacrylate. The resulting cell-laden array with a gradient of GelMA/PEG composition was used to screen human PDLSC response to ECM. The behavior (e.g., cell viability, spreading) of human PDLSCs in GelMA/PEG array were found to be depended on the volume ratios of GelMA/PEG, with cell viability and spreading area decreased along with increasing the ratio of PEG. The developed approach would be useful for screening cell-biomaterial interaction in 3D and promoting regeneration of functional tissue.

1. Introduction

Periodontitis is an inflammatory disease that causes destruction in tooth supporting structure, periodontal defect and eventually tooth loss, negatively affecting up to 15% of adults worldwide [1]. Although existing clinical therapies for periodontal disease (e.g., root surface conditioning, guided tissue regeneration) have shown benefits for controlling local inflammation of periodontium and the progression of periodontitis, they can not produce desirable tissue regeneration [2]. Recently, periodontal ligament (PDL) stem cells (PDLSCs) have been found to promote the formation of new bone, cementum and functional PDL in diseased periodontium under appropriate stimulation [3–5]. This shows the great promises of PDLSCs for periodontal tissue regeneration. Indeed, existing data indicate that PDLSCs are PDL-derived mesenchymal stem cells that possess many osteoblast/cementoblast-like properties, such as the capacity to form mineralized nodules, expression of bone/cementum-associated markers, and response to bone-inductive factors in vitro [6]. Accumulating evidence has shown that the behavior and fate of stem cells including PDLSCs are closely related to their microenvironment, which is mainly composed of extracellular matrix (ECM) and soluble factors [7–11]. As the structural and biochemical support for cells reside, ECM plays an important role on cell adhesion, migration, proliferation, differentiation and cell-cell communication [12–14]. However, the impact of the ECM composition on PDLSCs remains unclear. Therefore, it is of great importance to study PDLSC-ECM interaction to find idea ECM (e.g., composition, concentration) for PDLSCs.

Many types of biomaterials, including those based on natural and synthetic polymers, have been developed to mimic ECM for culturing cells and directing cell behaviors [15, 16]. However, ECM of different tissues, and even different locations in the same tissue, may vary in chemical composition, structural and mechanical properties. The diversity and specificity of ECMs make traditional individual design and

examination time consuming to screen for idea biomaterials. Therefore, microarray techniques have been explored to improve throughput by performing multiple tests in parallel [17–19]. Currently, most of the microarray platforms for screening cell-biomaterial interaction are based on two-dimensional (2D) substrates, which, however, may not represent native conditions as increasing evidences have indicated that cells behave differently in many aspects in three-dimensional (3D) culture [20, 21]. Methods such as soft lithography and photopatterning have thus been utilized to obtain cell-laden hydrogel arrays for screening cell-biomaterial interaction in 3D [22, 23]. However, they are more or less suffering from some limitations such as limited diverse controls of composition and mechanical characteristics in a single plate. Recently, the emerging and development of 3D bioprinting technologies showed their advantages in producing diverse cell-laden hydrogel microarrays on demand [24, 25], which may hold great potentials for cell-biomaterial interaction screening applications.

In this paper, we proposed a bioprinting-based approach to generate 3D cell-laden hydrogel array with gradient of ECM, through controlling the volume ratio of two hydrogels. We used photocrosslinkable gelatin methacrylate (GelMA) and poly(ethylene glycol) (PEG) dimethacrylate as example hydrogels to demonstrate the feasibility and effectiveness of our approach. We printed an array of GelMA/PEG hydrogel encapsulating human PDLSCs with a gradient of material composition and investigated the responses of human PDLSCs in the GelMA/PEG hydrogel array. The approach may be not only helpful for human PDLSCs-ECM screening but also for other cell-ECM systems.

2. Materials and methods

2.1. Materials

Poly(ethylene glycol) (PEG) dimethacrylate, gelatin (Type A, 300 bloom from porcine skin), methacrylic anhydride (MA) and 2-hydroxy-2-methylpropiophenone (TCI, photoinitiator) were purchased from SigmaeAldrich (Wisconsin, USA). GelMA was synthesized according to the previous descriptions [26]. UV light source used (Model XLE-1000 A/F) was manufactured at Spectroline (NY, USA). The concentration of GelMA and PEG used in the present study is 5 wt% and 10 wt% respectively.

2.2. Cell printing platform

In this study, we used a customer-designed pressure-assisted valve-based bioprinting system (figure 1(a)), which mainly consists of a 3D piezoceramics motion stage (KDT180-100-LM (XY) and MT105-50-LM (Z), Feinmess Dresden GmbH, Dresden, Germany), a solenoid valve ejector (G100–150300, TechElan, Mountainside, NJ, USA) and a digital pulse signal generator (Agilent 81101A, Test Equipment Connection, Lake Mary, FL, USA). The system is enclosed within a sterile hood and controlled by a computer. Our system provides a minimum dispense volume of 25 nl and a spatial resolution of 50 nm with about 2 μm of relative deviation. Pneumatic power source is used for ejecting cells, avoiding strong external stimulation (e.g., high shear force and temperature much over 37 °C). The volume of printed droplets can be tuned by the properties of the sample (e.g., surface tension, viscosity), the diameter of the nozzle orifice (diameter of 150 μm in this study), the valve opening duration (controlled by using a signal generator) and the inlet pressure.

2.3. Characterization of droplet size

For a given sample (i.e., fixed viscosity), we can tune the droplet size (i.e., volume) by changing the valve opening duration and the inlet pressure. To investigate the effect of valve opening duration on the droplet size, we fixed the inlet pressure at 50 kPa, while to study the influence of inlet pressure, we fixed the valve opening duration at 3 ms according to our previous studies [27]. To measure the droplet volume, 1000 droplets were printed into a small tube and then the total droplet volume was calculated through measuring the volume change in the reservoir. First, 1000 μl sample was put in the reservoir before printing. Then, 100, 10 and 2.5 μl pipettes were used to measure the rest sample volume after printing. Finally, the volume change in the reservoir was calculated and obtained. The reliability of this measurement was checked by repeat test. The volume per droplet can be obtained through the following calculation: droplet volume (nl) = total volume of sample (μl) $\times$ 10^3/number of droplets.

2.4. Isolation of primary cells from human PDL

PDL tissue specimens were obtained from healthy patients and used for tissue biopsy and PDL cell isolation. The samples were transported to the lab and placed in an alpha modification of Eagle's medium (α-MEM, Hyclone, Road Logan, UT, USA) with 10% fetal bovine serum (FBS) and 1% penicillin and streptomycin. The use of human periodontal tissue for research and all procedures was approved by the Ethics Committee in Xi'an Jiaotong University. Human PDLSCs were isolated and cultured, following previous literature with a few modifications [28]. Briefly, PDL tissues were collected, rinsed with PBS 4 times and placed in a tube and digested with α-MEM with 3 mg ml^{-1} collagenase (type I) and 4 mg ml^{-1} dispase (Roche Diagnostics, USA) for 20 min at 37 °C with continuous shaking. Then the tissues were transferred to the Petri dishes containing the modified α-MEM (10% FBS and 100 units ml^{-1} penicillin streptomycin). These tissues were placed in an incubator with

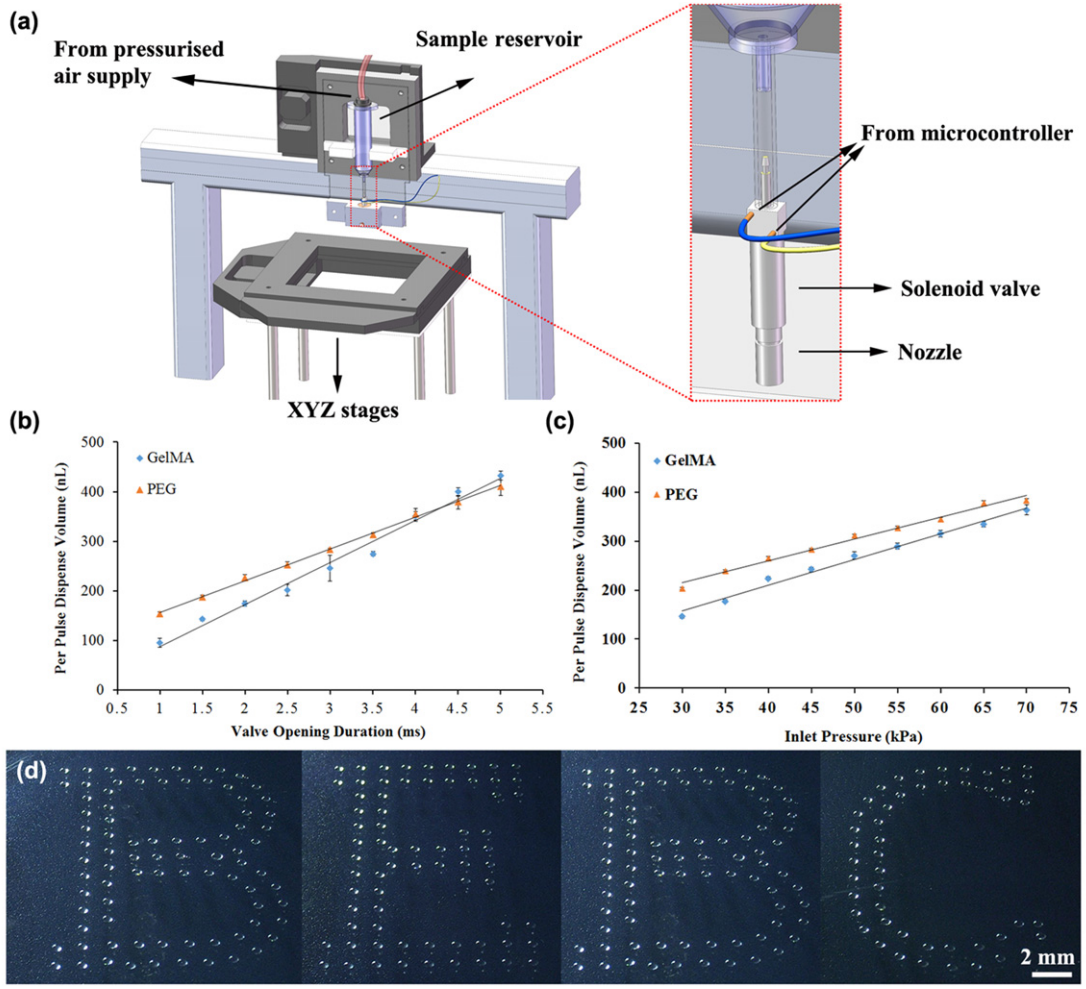

Figure 1. Bioprinting platform and characterization of droplet printing. (a) Schematic drawing of the bioprinting platform and detailed schematic of the valve-based nozzle. (b) Curves of droplet volumes at different valve opening duration. (c) Curves of droplet volumes at various pressures. (d) Image of a pattern printing in the form of the abbreviation of our center (BEBC).

5% CO_2 at 37 °C until cells grew out from the tissue pieces.

2.5. Single-cell cloning

Single-cell cloning was achieved by the limiting dilution method, following the protocol from the literature [28]. In brief, we collected the cells that grew out from PDL tissue, which were suspended and diluted with a concentration of 10 cells ml^{-1}. 100 μl diluted suspensions was seeded in each well of a 96-well plate. Wells containing the separated and single cells were chosen by visual observation via microscopy. After the cells grew 80% confluence, they were harvested for further enlarged culture. These cells were regarded as passage 1 (P1) for PDLSCs, and cells at P3–P5 were used in this study to avoid potential changes in cell behavior (e.g., cell viability) as induced by over proliferation [29].

2.6. Flow cytometric analysis

To determine the expression of the conventional surface markers of human mesenchymal stem cells, CD29, CD31, CD45 and CD90 (affymetrix eBiosciences, USA) were examined by flow cytometry. Human PDLSCs were prepared as cell suspensions and resuspended in PBS buffer. Approximately 1×10^6 cells ml^{-1} were incubated with phycoerythrin (PE)- or fluorescein isothiocyanate (FITC)-conjugated monoclonal antibodies against CD29, CD31, CD45 and CD90 for at least 20 min at 4 °C in the dark. Then they were rinsed by PBS via centrifugation (4 °C, 1000 rpm, 5 min) for 2 times and kept in PBS on ice until analysis. All samples were analyzed via BD Canto flow cytometer (Becton, Dickinson Company, USA). Data were processed using FACSDiva Version 6.1.3 software (Becton, Dickinson Company, USA).

2.7. Cell viability

The short-term cell viability (i.e., immediately after printing) was assessed via Trypan Blue exclusion (T8154, Sigma-Aldrich). In brief, human PDLSCs were suspended in α-MEM at a concentration of 1×10^5 cells ml^{-1}. Then this cell suspension was loaded into the cell printer and printed onto different Petri dishes with a range of inlet pressures (40, 45, 50, 55, 60 kPa). The control (cells not printed) was created

in Petri dish by manual pipetting. Trypan Blue was used in these samples to stain the dead cells before being examined under the microscope (Olympus IX 81, Olympus, USA). Five random samples taken from each printed and control groups were loaded on hemocytometer and examined. The number of live cells and dead cells were manually counted under the microscope.

The long-term cell viability (i.e., 24 and 72 h after printing) was assessed by live/dead staining. For this, a cell suspension of human PDLSCs at a concentration of approximately 1×10^6 cells ml^{-1} in α-MEM was loaded into the reservoir of cell printer. A control was obtained from the unprinted cell/α-MEM suspension. In the printed group, cell/α-MEM suspension was printed with varying inlet pressures (40, 45, 50, 55, 60 kPa). The samples were stained by calcein and ethidium bromide (LIVE/DEAD® Viability/Cytotoxicity Kit, USA) at 24 and 72 h after printing and the numbers of live and dead cells were counted via ImageJ through the obtained bright-field images taken using (LSM700, ZEISS, USA).

2.8. CD90 and CD29 immunofluorescence

Human PDLSC cells were printed at the pressure of 40 and 60 kPa (representing the minimum and maximum pressure used in our study), and then cultured in incubator for 72 h. The adherent human PDLSCs were washed twice with PBS at room temperature. After that, 25 μl anti-human CD90 FITC (affymetrix eBiosciences, USA) and 25 μl anti-human CD29 PE (affymetrix eBiosciences, USA) were added to 500 μl PBS and mixed. Cell samples were stained with this solution for 30 min at 4 °C and kept away from light. Then they were rinsed by PBS for 3 times and kept in PBS. The CD90 and CD29 immunofluorescence were imaged using fluorescence microscope.

2.9. Combinatorial printing for screening of human PDLSCs responses to ECM

Combinatorial printing of 3D cell-laden hydrogels was designed, basing on some previous literatures with the modifications [30, 31]. Generally, the bioprinter can be integrated with multiple valves, each of which can be connected with separate sample reservoirs containing different bio-inks. The first sample reservoir was loaded with cells resuspended in GelMA containing 0.5% (w/v) photoinitiator at a concentration of 1×10^6 cells ml^{-1}, while the second reservoir was loaded with cells/PEG suspension and photoinitiator at the same cell concentration. An array of droplets (6×6) containing cells/GelMA was first printed with decreasing droplet size, creating a gradient of droplet sizes. Then, an opposing gradient of cells/PEG droplets was printed over the existing array, leading to an array of droplets with uniform size and a gradient of droplet composition (GelMA/PEG volume ratio: 5/0, 4/1, 3/2, 2/3, 1/4 and 0/5). The completed array was then exposed to 2.9 mW cm^{-2} UV light (365 nm) for 30 s to form a cell-laden GelMA/PEG hydrogel array. Finally, cell-laden hydrogel array was cultured in incubator. After 3 day culture, cell viability and cell spreading area of the human PDLSCs encapsulated in hydrogels with different composition was determined. Cell viability was calculated through 2D images of 3D structures taken by fluorescence microscope. For each sample, the images at several layers along the thickness of the hydrogel were taken. Hence, one of these images from each sample was used to show the cell viability qualitatively, while the quantitative data were obtained by processing the images via ImageJ software. Cell spreading area was obtained as follows. Briefly, Cell number and single cell area could be counted by ImageJ software directly. Then the total cell area could be calculated. Actually, cell area was counted by this software in the unit of pixel point. According to the relation between scale bar and pixel point, we could calculate the total cell area in the unit of μm^2. Finally, the cell area could be obtained through the following calculation: cell area (μm^2) = total cell area (μm^2)/cell number.

2.10. CCK-8 assay for proliferation

A cell count kit-8 (CCK-8, 7sea biotech, China) was used to quantitatively evaluate the cell proliferation. At days 3 and 5 after printing, CCK-8 with a 10 vol% of the medium was added to the samples and incubated for 4 h at 37 °C. CCK-8 was transformed into orange-colored formazan by the activity of dehydrogenases in cells. The amount of formazan is directly proportional to the number of living cells. 100 μl of the reaction solution was transferred into a new 96-well plate and the absorbance (OD) of the solution was measured by a microplate reader (Biorad, USA) at 450 nm. The experiments were carried out in sextuplicate.

3. Results and discussion

3.1. Characterization of droplet printing

In this study, we proposed a bioprinting-based approach to generate 3D cell-laden hydrogel array with gradient of ECM, through controlling the volume ratio of two hydrogels (i.e., GelMA and PEG). Since our approach is based on the precise control of droplet volume to create such array with ECM gradient, we first characterized the volume of printed droplet for both GelMA and PEG under different valve opening duration and inlet pressure (figures 1(b)–(c)). We observed that the volume per droplet increased linearly with increasing valve opening duration and inlet pressure for both GelMA and PEG. For instance, the minimum and maximum volume per droplet of GelMA is 95 ± 9 and 433 ± 9 nl by tuning valve opening duration in the range of 1–5 ms. While the minimum and maximum volume per droplet of GelMA is 146 ± 3 and 364 ± 11 nl via controlling

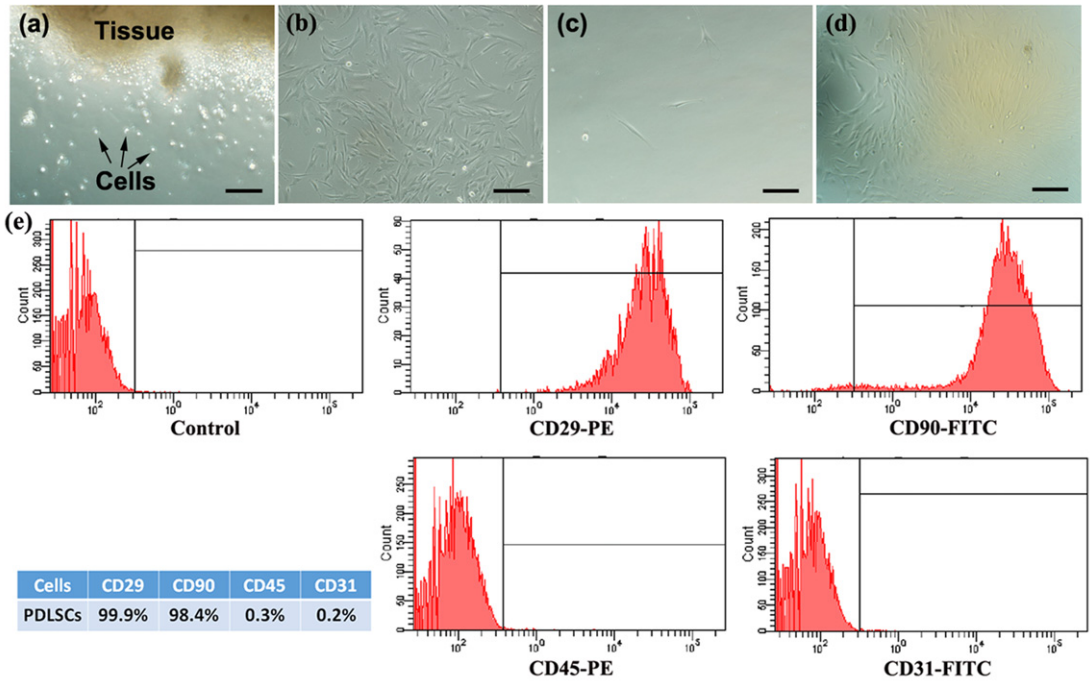

Figure 2. Primary cell culture, single-cell cloning and characterization of human PDLSCs. Primary cell growth, single-cell cloning and characterization of human PDLSCs. Microscopy images of primary cells grown from human periodontal ligament tissue at (a) day 4 and (b) day 21. Microscopy images of single-cell cloning and cell proliferation at (c) 12 h and (d) day 3, respectively. (e) Results from flow cytometric analysis. Scale bar: 200 μm.

inlet pressure in the range of 30–70 kPa. Under most conditions used in this study, PEG droplet size is larger than GelMA, which is mainly due to the difference in the viscosity of the printed hydrogels. These results indicate that we can precisely control the droplet size in the range of 100–450 nl by tuning the inlet pressure and valve opening duration. Besides, we did not observe obvious difference on droplet size for sample with and without cells (data not shown). To demonstrate the precision of our cell printer, we printed the abbreviation of center name (i.e., 'BEBC'), figure 1(d).

3.2. Primary cell growth, single-cell cloning and characterization of human PDLSCs

To obtain the human PDLSCs, primary cell culture was first carried out by using human PDL tissues (figure 2). We observed that the initial primary cells derived from PDL tissue show round shape after culturing the transferred tissues for 4 d (figure 2(a)). These primary cells reached 90% confluence by 21 d, which exhibited the spindle-shaped and fibroblast-like morphology (figure 2(b)). Since PDLSCs are often enriched with fibroblasts, single-cell cloning (regarded as a common method) was used to separate human PDLSCs from fibroblasts. For single-cell colonies, the primary adherent cells were detached from the Petri dish and suspended in culture medium, which were then seeded in 96-well plate. We used wells containing only single cells and found that the cells tightly adhered to the plate bottom after culture for 12 h (figure 2(c)). After 3 day culture, these cells grew 80% confluence and displayed a spindle-shaped fibroblast-like (figure 2(d)), which is similar to cell morphology of PDLSCs observed in literature [3, 29]. To further confirm the obtained cells above are human PDLSCs, we carried out immunophenotype characterization from culture at P3–P5 by flow cytometric analysis (figure 2(e)). We found that the cells positively expressed mesenchymal stem cell markers including CD29 and CD90, but were negative for endothelial cells marker (CD31) and the hematopoietic stem cells marker (CD45). The *in vitro* cell phenotypes of human PDLSCs were similar to those reported in literature [5, 29]. All these results demonstrate that human PDLSCs were successfully obtained.

3.3. Characterization of cell viability and functionality after printing

To determine whether the printing process has an immediate damage on cells, we measured the short-term cell viability (figure 3(a)). We found that cells maintained high viability (>94%) using our valve-based cell printer in the pressure range (40–60 kPa). This indicates that the printing process did not induce immediate damage to the cells. We further examined cell viability with a long-term investigation at 24 and 72 h post printing (figure 3(b)). The cellular viability was calculated to be 95.1% $\pm$ 3.2 after 24 h and about 82.4% $\pm$ 4.7% after 72 h culture for all pressures. It confirms that our cell printing process does not have significant effect on the long-term viability of human PDLSCs, which is consistent with our previous studies

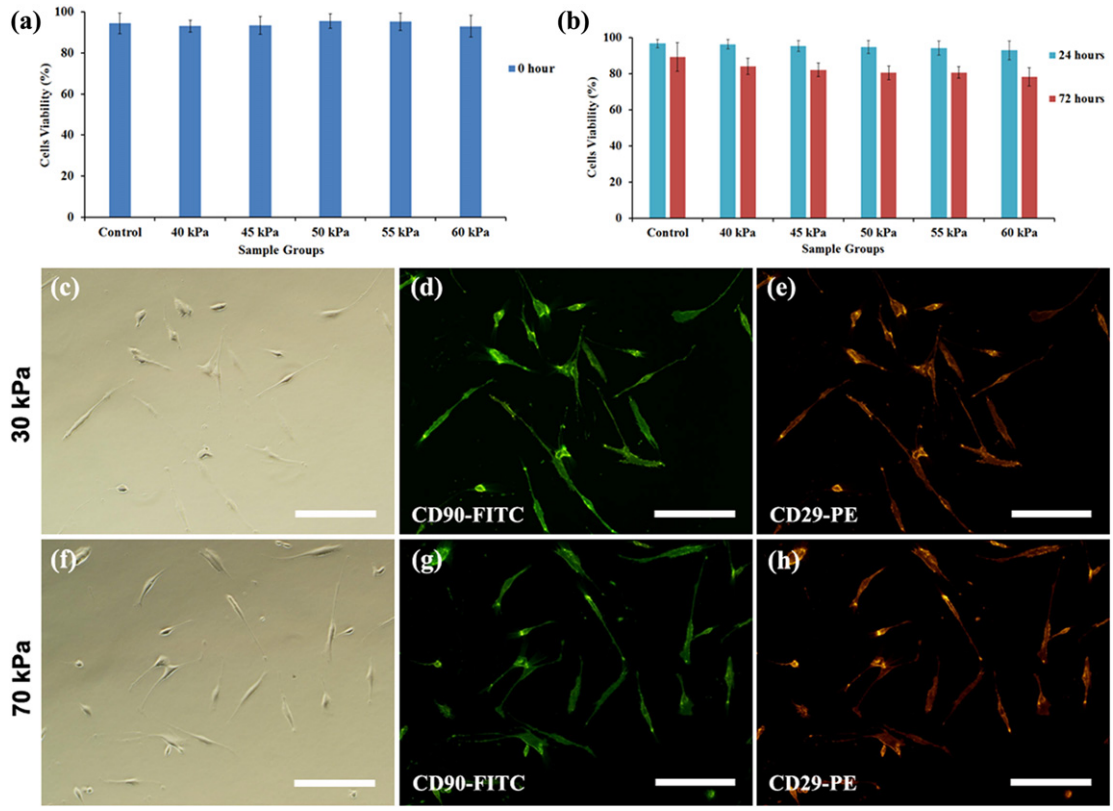

Figure 3. Characterization of cell viability and functionality after printing. (a) Percentages of live cells after immediate printing. (b) Cell viability as a function of pressure at 24 and 72 h post printing. (c) Fluorescence image of the printed human PDLSCs after 72 h culture. Scale bar: 200 μm.

on other cell types [27, 32]. To investigate the effect of printing procedure on the multipotency of human PDLSCs, we further checked the functionality of human PDLSCs after printing for 72 h (figures 3(c)–(h)). We observed that human PDLSCs remained positive for both CD29 and CD90 antibody (figures 3(d)–(e) and (g)–(h)) but negative for CD31 and CD45 antibody (data not shown), indicating that the printing process does not affect the multipotency of human PDLSCs.

3.4. Combinatorial printing for screening of human PDLSCs responses to ECM

To increase the throughput capability of screening cell-ECM interaction, it is necessary to print arrays with gradients of ECM composition and concentration. For this, an array of cells/GelMA droplets was first printed with decreasing droplet size to create an array with a gradient of droplet volume (figure 4(b)). Then an opposing gradient of cells/PEG droplets were printed over the existing array, resulting in an array of droplets with uniform size and a gradient of composition in GelMA/PEG (figure 4(c)). A GelMA/PEG droplet array containing human PDLSCs with a gradient of composition (GelMA/PEG volume ratio: 5/0, 4/1, 3/2, 2/3, 1/4 and 0/5) was created first. Human PDLSCs were encapsulated in GelMA/PEG hydrogels at uniform cell concentration by UV photopolymerization.

We first checked the viability of human PDLSCs in hydrogels with different GelMA/PEG ratio after 3 day culture. From live/dead staining, we observed that human PDLSCs encapsulated in GelMA/PEG hydrogels remained viable for all six compositions (figures 4(d)–(i)). We then quantified the cell viability by counting the number of live and dead cells. We found that cell viability decreased significantly with increasing volume ratio of PEG (figure 4(j)). Cell viability at day 3 after printing was 82.5% $\pm$ 4.1% in hydrogels with the GelMA/PEG volume ratio of 5/0, which was obviously higher than that of 0/5 (30%) hydrogel samples. Our observation is in agreement with the previous study where embryoid bodies encapsulated in PEG hydrogels reduced cell growth, while in GelMA hydrogels, higher call viability was obtained [33]. This may be attributed to that GelMA and PEG exhibit different bioactivities, where the biodegradable GelMA is capable of mediating cell adhesion, proliferation and differentiation while PEG hydrogels are nondegradable and chemically inert [34].

In addition, after culture for 3 d, human PDLSCs spread and elongated in first three hydrogels (GelMA/PEG volume ratio: 5/0, 4/1 and 3/2), which varied inversely with the increase in volume ratio of PEG

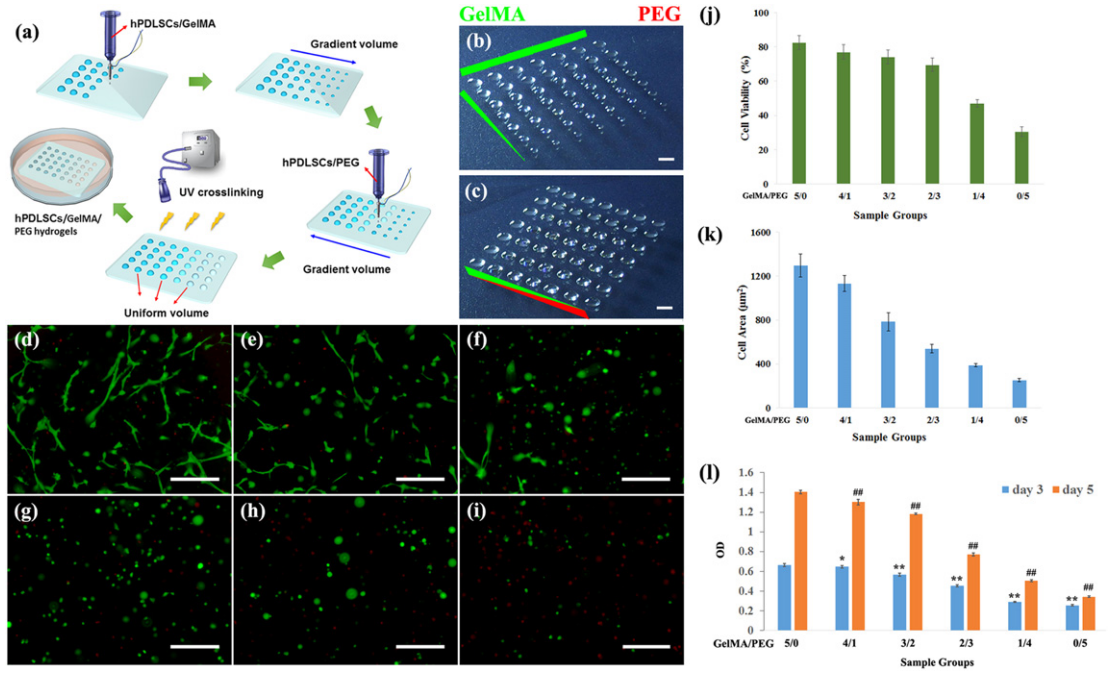

Figure 4. Combinatorial printing for screening of human PDLSCs responses to ECM. (a) Schematic of bioprinting 3D cell-laden hydrogel array for screening human PDLSCs response to ECM. (b) An array of human PDLSCs/GelMA with a gradient of droplet volume. (c) The same array with an opposing gradient of human PDLSCs/PEG overprinted to creat uniform volume droplets with a gradient GelMA/PEG ratio. Human PDLSCs encapsulated in 3D hydrogels with a gradient of GelMA/PEG ratio (v/v) were stained via LIVE/DEAD assay 72 h after printing; GelMA/PEG ratio: (d) 5:0, (e) 4:1, (f) 3:2, (g) 2:3, (h) 1:4 and (i) 0:5. Scale bar: 200 μm. (j) Cell viability calculated from (d) to (i). (k) Cell area calculated from (d) to (i). (l) CCK-8 assay of human PDLSCs cultured in different hydrogels with gradient compositions on days 3 and 5. Data were expressed as means $\pm$ standard deviation (SD) ($n = 6$ for each sample). Single asterisk (*) and double asterisk (**) denote a statistical significance of $p < 0.05$ and $p < 0.01$, respectively, compared to data obtained from 5/0 sample on day 3. Double pound sign (##) denotes a statistical significance of $p < 0.01$, compared to data obtained from 5/0 sample on day 5.

(figures 4(d)–(f)). Especially, in 5/0 (GelMa/PEG, v/v) hydrogel, cells spread, elongated and formed interconnected networks with neighboring cells. While in the last three hydrogels (GelMA/PEG volume ratio: 2/3, 1/4 and 0/5), human PDLSCs did not spread and elongate any more, just appeared in round shape (figures 4(g)–(i)). We also quantified cell spreading area using ImageJ and found that cell area reduced dramatically with decrease in GelMA and increase in PEG volume ratio concurrently (figure 4(k)). To evaluate the effect of ECM compositions on human PDLSCs proliferation, the CCK-8 tests were carried out to determine the viable cells number quantitatively in CelMA/PEG hydrogels with different materials compositions on days 3 and 5 after printing. As shown in figure 4(l), similar trends were found in these hydrogels with gradient compositions. The number of viable human PDLSCs increased from days 3 to 5 within all samples. Moreover, the viable cells decreased with decreasing volume ratio of GelMA both on days 3 and 5. Statistically, on day 3, there is a significant difference between 5/0 and 4/1 samples ($p < 0.05$), while there exists the significant differences among 5/0, 3/2, 2/3, 1/4 and 0/5 samples ($p < 0.01$). In contrast, on day 5, there are significant differences among all samples ($p < 0.01$), indicating that the hydrogel composition with more PEG has an inhibitory effect on the proliferation of human PDLSCs.

For recreating native tissue morphology in engineered tissues, it is of great importance to enhance the ability of cells to spread, elongate, proliferate and connect with neighboring cells in 3D [26]. Encapsulating cells in hydrogel containing PEG allows for homogeneous cell distribution with maintained cell viability to some extent. However, cells encapsulated in these hydrogels are generally unable to bind to the hydrogel network limiting their utility in engineered tissues. One advantage of GelMA is the presence of binding sites distributed throughout the hydrogel on all polymer chains, which could potentially improve the cell binding. Cells can easily bind to, spread and proliferate within GelMA demonstrating its positive cell-binding behavior. Therefore, the addition of binding motifs can improves cell binding and proliferation, through either incorporation of cell-adhesive peptide sequences [12, 13, 35, 36] or mixing with native ECM components [37] and other naturally derived proteins (e.g., fibrin) [38].

Besides, most existing studies on cell-ECM interaction only examined ECM component in isolation, which cannot recapitulate native situation and fails to capture interaction effects between ECM components, leading to discrepancies between *in vitro* and *in vivo*

cell behaviors. Our approach is based on bioprinting, which holds great potential for high-throughput characterization and optimization of cellular interactions with their microenvironments. Compared to conventional approaches where single ECM component is tested individually, screening combinatorial biomaterial libraries based on the printed gradient array could result in the discovery of unexpected material solutions to these complex problems [39] and optimization of stem cell microenvironments to control cell behaviors [40].

4. Conclusions

In this study, we proposed a bioprinting-based approach to generate cell-laden hydrogel array with gradient composition for screening cell-ECM interaction in 3D. As a first verification, we printed GelMA and PEG sequentially to obtain hydrogel array with gradient composition by tuning the volume ratios of GelMA-to-PEG. The viability and multipotency of human PDLSCs were maintained during isolation and printing process. The behavior (e.g., cell viability, spreading) of human PDLSCs in GelMA/PEG array were found to be depended on the volume ratio of GelMA-to-PEG, where cell viability and spreading area decreased along with increasing ratio of PEG. The developed approach would be useful for screening cell-biomaterial interaction in 3D and promoting regeneration of functional tissue.

Acknowledgments

This work was financially supported by the National Natural Science Foundation of China (51502238, 11372243), the Fundamental Research Funds for the Central Universities (xjj2015052), China Postdoctoral Science Foundation (2015M572569), and the Project Supported by Natural Science Basic Research Plan in Shaanxi Province of China (2014JQ1004). All the work was performed at XJTU Bioinspired Engineering and Biomechanics Center.

References

[1] Albandar J M 2005 Epidemiology and risk factors of periodontal diseases *Dent. Clin. North Am.* **49** 517–32
[2] Chen F M, Zhang J, Zhang M, An Y, Chen F and Wu Z-F 2010 A review on endogenous regenerative technology in periodontal regenerative medicine *Bioanalysis* **31** 7892–927
[3] Liu Y, Zheng Y, Ding G, Fang D, Zhang C, Bartold P M, Gronthos S, Shi S and Wang S 2008 Periodontal ligament stem cell-mediated treatment for periodontitis in miniature swine *Stem Cells* **26** 1065–73
[4] Park J Y, Jeon S H and Choung P H 2011 Efficacy of periodontal stem cell transplantation in the treatment of advanced periodontitis *Cell Transplant.* **20** 271–85
[5] Tsumanuma Y *et al* 2011 Comparison of different tissue-derived stem cell sheets for periodontal regeneration in a canine 1-wall defect model *Bioanalysis* **32** 5819–25
[6] Seo B M, Miura M, Gronthos S, Bartold P M, Batouli S, Brahim J, Young M, Robey P G, Wang C Y and Shi S T 2004 Investigation of multipotent postnatal stem cells from human periodontal ligament *Lancet* **364** 149–55
[7] Hacking S A and Khademhosseini A 2009 Applications of microscale technologies for regenerative dentistry *J. Dent. Res.* **88** 409–21
[8] Huang S S, Tam V, Cheung K M C, Long D, Lv M M, Wang T and Zhou G Q 2011 Stem cell-based approaches for intervertebral disc regeneration *Curr. Stem Cell Res. Ther.* **6** 317–26
[9] Yamamoto T, Ugawa Y, Yamashiro K, Shimoe M, Tomikawa K, Hongo S, Kochi S, Ideguchi H, Maeda H and Takashiba S 2014 Osteogenic differentiation regulated by Rho-kinase in periodontal ligament cells *Differentiation* **88** 33–41
[10] Yang Z H, Jin F, Zhang X J, Ma D D, Han C, Huo N, Wang Y X, Zhang Y F, Lin Z and Jin Y 2009 Tissue engineering of cementum/periodontal-ligament complex using a novel three-dimensional pellet cultivation system for human periodontal ligament stem cells *Tissue Eng.* C **15** 571–81
[11] Yu N, Prodanov L, te Riet J, Yang F, Walboomers X F and Jansen J A 2013 Regulation of periodontal ligament cell behavior by cyclic mechanical loading and substrate nanotexture *J. Periodontol.* **84** 1504–13
[12] Mann B K, Gobin A S, Tsai A T, Schmedlen R H and West J L 2001 Smooth muscle cell growth in photopolymerized hydrogels with cell adhesive and proteolytically degradable domains: synthetic ECM analogs for tissue engineering *Bioanalysis* **22** 3045–51
[13] Mann B K and West J L 2002 Cell adhesion peptides alter smooth muscle cell adhesion, proliferation, migration, and matrix protein synthesis on modified surfaces and in polymer scaffolds *J. Biomed. Mater. Res.* **60** 86–93
[14] Gobin A S and West J L 2002 Cell migration through defined, synthetic ECM analogs *FASEB J.* **16** 751–3
[15] Geckil H, Xu F, Zhang X, Moon S and Demirci U 2010 Engineering hydrogels as extracellular matrix mimics *Nanomedicine* **5** 469–84
[16] Li Y, Huang G, Zhang X, Li B, Chen Y, Lu T, Lu T J and Xu F 2013 Magnetic hydrogels and their potential biomedical applications *Adv. Funct. Mater.* **23** 660–72
[17] Yliperttula M, Chung B G, Navaladi A, Manbachi A and Urtti A 2008 High-throughput screening of cell responses to biomaterials *Eur. J. Pharm. Sci.* **35** 151–60
[18] Rozkiewicz D I, Kraan Y, Werten M W, de Wolf F A, Subramaniam V, Ravoo B J and Reinhoudt D N 2006 Covalent microcontact printing of proteins for cell patterning *Chem. Eur. J.* **12** 6290–7
[19] Flaim C J, Chien S and Bhatia S N 2005 An extracellular matrix microarray for probing cellular differentiation *Nat. Methods* **2** 119–25
[20] Loessner D, Stok K S, Lutolf M P, Hutmacher D W, Clements J A and Rizzi S C 2010 Bioengineered 3D platform to explore cell–ECM interactions and drug resistance of epithelial ovarian cancer cells *Bioanalysis* **31** 8494–506
[21] Zorlutuna P, Annabi N, Camci-Unal G, Nikkhah M, Cha J M, Nichol J W, Manbachi A, Bae H, Chen S and Khademhosseini A 2012 Microfabricated biomaterials for engineering 3D tissues *Adv. Mater.* **24** 1782–804
[22] Oliveira M B and Mano J F 2014 High-throughput screening for integrative biomaterials design: exploring advances and new trends *Trends Biotechnol.* **32** 627–36
[23] Li X, Valadez A V, Zuo P and Nie Z 2012 Microfluidic 3D cell culture: potential application for tissue-based bioassays *Bioanalysis* **4** 1509–25
[24] Yoo S S and Polio S 2010 *Cell and Organ Printing* (Berlin: Springer) pp 3–19
[25] Murphy S V and Atala A 2014 3D bioprinting of tissues and organs *Nat. Biotechnol.* **32** 773–85
[26] Nichol J W, Koshy S T, Bae H, Hwang C M, Yamanlar S and Khademhosseini A 2010 Cell-laden microengineered gelatin methacrylate hydrogels *Bioanalysis* **31** 5536–44

[27] Xu F, Celli J, Rizvi I, Moon S, Hasan T and Demirci U 2011 A three-dimensional in vitro ovarian cancer coculture model using a high-throughput cell patterning platform *Biotechnol. J.* **6** 204–12
[28] Zhang J, An Y, Gao L N, Zhang Y J, Jin Y and Chen F M 2012 The effect of aging on the pluripotential capacity and regenerative potential of human periodontal ligament stem cells *Bioanalysis* **33** 6974–86
[29] Yang H, Gao L N, An Y, Hu C H, Jin F, Zhou J, Jin Y and Chen F M 2013 Comparison of mesenchymal stem cells derived from gingival tissue and periodontal ligament in different incubation conditions *Bioanalysis* **34** 7033–47
[30] Xu F, Sridharan B, Wang S Q, Gurkan U A, Syverud B and Demirci U 2011 Embryonic stem cell bioprinting for uniform and controlled size embryoid body formation *Biomicrofluidics* **5** 022207
[31] Li C *et al* 2015 Rapid formation of a supramolecular polypeptide-DNA hydrogel for *in situ* three-dimensional multilayer bioprinting *Angew. Chem.-Int. Ed.* **54** 3957–61
[32] Moon S, Lin P A, Keles H O, Yoo S S and Demirci U 2007 Title cell encapsulation by droplets *J. Vis. Exp.* **8** 316–316
[33] Qi H, Du Y A, Wang L Y, Kaji H, Bae H J and Khademhosseini A 2010 Patterned differentiation of individual embryoid bodies in spatially organized 3D hybrid microgels *Adv. Mater.* **22** 5276–81
[34] Sawhney A S, Pathak C P and Hubbell J A 1993 Interfacial photopolymerization of poly(ethylene glycol)-based hydrogels upon alginate poly(l-lysine) microcapsules for enhanced biocompatibility *Bioanalysis* **14** 1008–16
[35] Tsang V L, Chen A A, Cho L M, Jadin K D, Sah R L, DeLong S, West J L and Bhatia S N 2007 Fabrication of 3D hepatic tissues by additive photopatterning of cellular hydrogels *Faseb J.* **21** 790–801
[36] Schmedlen K H, Masters K S and West J L 2002 Photocrosslinkable polyvinyl alcohol hydrogels that can be modified with cell adhesion peptides for use in tissue engineering *Bioanalysis* **23** 4325–32
[37] Brigham M D, Bick A, Lo E, Bendali A, Burdick J A and Khademhosseini A 2009 Mechanically robust and bioadhesive collagen and photocrosslinkable hyaluronic acid semi-interpenetrating networks *Tissue Eng.* A **15** 1645–53
[38] Dikovsky D, Bianco-Peled H and Seliktar D 2006 The effect of structural alterations of PEG-fibrinogen hydrogel scaffolds on 3D cellular morphology and cellular migration *Bioanalysis* **27** 1496–506
[39] Hook A L, Anderson D G, Langer R, Williams P, Davies M C and Alexander M R 2010 High throughput methods applied in biomaterial development and discovery *Biomaterials* **31** 187–98
[40] Yang F, Mei Y, Langer R and Anderson D G 2009 High throughput optimization of stem cell microenvironments *Comb. Chem. High Throughput Screen* **12** 554–61